Voltage-Induced Frequency Disturbance Analysis Considering Fault Type and Network Location

Jie Song
KU Leuven & ETCH-EnergyVille
Leuven, Belgium
jie.song@kuleuven.be

Mehdi Ghazavi Dozein
Monash University
Melbourne, Australia
mehdi.ghazavidozein@monash.edu

Jef Beerten
KU Leuven & ETCH-EnergyVille
Leuven, Belgium
jef.beerten@kuleuven.be

***Abstract*—This paper investigates the voltage-induced frequency disturbance phenomenon that may happen during fault ride-through operation of inverter-based resources (IBRs) in low-inertia power systems. ETM simulations have been performed in the context of a grid-connected PV power plant (PVPP) where PV inverters are equipped with system support control and current limitation. Simulation case studies show that frequency variations can be triggered following short-circuit faults, associated with IBR active power reduction/cessation and converter current saturation. Among different types of faults, a balanced three-phase-to-ground fault stands for the most critical condition that poses severe frequency disturbances to the system. With regard to downstream faults within the IBR plant, there is a chance of reverse power flow due to high power losses in the internal medium voltage (MV) collection grid, which raises the non-compliance issue in the IBR plant performance. The presented complexities and the associated risk of cascading failures should be carefully considered by system operators and IBR project developers.**

***Index Terms*—Voltage-induced Frequency Disturbance, Fault Ride-through, Cascading Failure, Inverter Current Limitation, Reactive Power Prioritization.**

I. Introduction

Massive grid integration of inverter-based resources (IBRs) such as wind and solar PV units is changing the nature of modern power systems [1]. As a result, grid dynamic characteristics are dominated by power converter control from IBRs instead of the inherent physical feature of conventional synchronous generators (SGs) [2]. One particular feature that distinguishes IBRs from SGs is that they have to limit the current under disturbances following a current saturation function implemented in their control to protect themselves from being overloaded [3]. Such current saturation must be considered for short-circuit analysis where several or all IBRs are likely to hit their current limits [4].

Short-circuit behavior in IBR-rich power systems has been extensively studied, with prior work largely focusing on improving the fidelity of IBR responses and control actions during faults. Existing models capture key nonlinearities such as voltage-support control and current saturation [5], and transient stability from phase-locked loop (PLL) under short-circuit conditions [6]. Complementary control-oriented studies have proposed enhanced fault ride-through strategies with a direct-current-synchronization loop [7]. To enable system-level fault studies, reduced-order and dynamic equivalent representations have also been proposed, including fault-level-dependent impedance equivalents that reproduce the aggregate response of the studied system [8]. Although many aspects related to short-circuit analysis have been covered in the references for IBR-rich power systems, existing studies typically assume a constant grid frequency when formulating the system under fault conditions, which might not be a case in emerging power systems with a high share of IBRs and a reduced level of system inertia.

Voltage-induced frequency disturbance refers to the system frequency deviations from the nominal value due to a sudden power mismatch initiated by a voltage disturbance (e.g., short-circuit faults) [9]. The primary triggering factor is the temporary reduction of IBR active power during fault ride-through operation due to voltage fault ride-through and current saturation in response to voltage drop [10]. Such phenomena has already been observed in Tasmanian grid [11]. The British transmission system operator, NESO, has also pointed out that there is an increasing risk of frequency instability induced by voltage disturbances in systems with a high IBR penetration ratio [12]. In this direction, the literature has explored modeling and mitigation of voltage-induced frequency excursions, including studies on active-power trajectory models for wind turbines during fault ride-through operation [13], fault-induced frequency nadirs across various wind penetration levels [14], dispatch strategies that maximize wind-farm active power to limit post-fault frequency excursions [15], and low-voltage ride-through controls for offshore wind plants that accelerate active power recovery following fault clearance [16]. However, existing studies largely emphasize the potential severity of such issues without systematically analyzing how the type and location of a voltage disturbance may impact the extent and magnitude of voltage-induced frequency disturbances.

To gain a more comprehensive understanding on this under-explored topic, this paper conducts voltage-induced frequency disturbance analysis considering fault type and location. The studied system has been defined in a grid-connected PV power plant (PVPP) where the grid-support operation and current limitation from PV inverters as well as main grid frequency dynamics are considered. The paper fills the research gap of existing literature by: 1) investigating frequency dynamics

This work has been supported by Horizon Europe MSCA postdoctoral fellowship under grant 101153248 (EQUATOR).

979-8-3315-8138-1

induced by different types of short-circuit fault; 2) analyzing the system response with a fault appears in the MV collection grid.

II. Modeling Foundations for Voltage-Induced Frequency Disturbance Studies

A. Simplified Power System Modeling for Voltage-induced Frequency Disturbance Analysis

In this paper, we investigate the voltage-induced frequency disturbance phenomenon, with a focus on the grid-connected PVPP with multiple PV panels and several internal feeders interfaced with the external grid through one point of connection (PoC), e.g., the system under study in this paper, as the scheme shown in Fig. 1. In the context of voltage-induced frequency disturbance analysis, the main AC grid can be represented via a voltage source, $\underline{u}_{th}$, behind an equivalent impedance, $\underline{z}_{th}$. Unlike conventional Thévenin equivalent, which assumes a constant frequency for its internal voltage source, the grid frequency dynamics must be considered in voltage-induced frequency disturbance analysis. In this work, we consider the aggregated swing equation to capture overall system frequency dynamics, as follows:

$$\Delta p(t) = 2H_{eq}\frac{d\Delta f}{dt} + D_{eq}\Delta f(t) \tag{1}$$

where H_{eq} and D_{eq} are the aggregated inertia constant and damping coefficient of external power system, respectively. The power imbalance triggered by a disturbance (e.g., short-circuit faults in this work), $\Delta p(t)$, can be expressed as follows:

$$\Delta p(t) = p_{ME}(t) + p_{PoC}(t) \tag{2}$$

where p_{PoC} is the electrical power injected from the PVPP into the main AC grid at the PoC and $p_{ME}(t)$ is the mechanical power input to the aggregated synchronous machine. The mechanical power is typically regulated via the primary frequency droop control, which can be expressed as follows:

$$\Delta p_{ME}(t) + \tau_{eq}\frac{\Delta p_{ME}(t)}{dt} = -k_{pf}\Delta f(t) \tag{3}$$

where τ_{eq} and k_{pf} are the equivalent time constant and $p-f$ droop gain of the aggregated SG governor system, respectively. So, one can conclude that the modeling inertia and primary frequency control are essential for voltage-induced frequency disturbance analysis.

B. PV Inverter Modeling and Ride-through Operation

Each PV module is modeled with the grid-side PV inverter (PVI), which operates in grid-following (GFL) mode with a PQ control. The PV inverter (PVI) operation during the fault follows the equivalent model expressed in [17]. The following settings on inverter fault ride-through operation are briefly explained in this paper as they are essentially for consideration in voltage-induced frequency disturbance analysis:

- **Negative sequence current control:** this paper assumes no negative sequence current injection from PV inverters (i.e., $\underline{i}^- = 0$). This assumption holds for legacy inverters who do not have grid-support functionality in negative sequence.
- **Positive sequence current control:** During the fault, the PV inverter follows the same active power reference as in pre-fault operating point, while the reactive power controller output, i^+_{d0}, is frozen and a fast reactive current injection is activated in the form of voltage-droop response. The consequent PV inverter setpoint in positive sequence can thus be expressed as follows:

$$p^+_{ref} = p^+_{disp};\ q^+_{ref} = u^+[i^+_{d0} + k_{isp}(u^+_{ref} - u^+)] \tag{4}$$

where p^+_{ref} and q^+_{ref} are the PV inverter active and reactive power setpoints in positive sequence, p^+_{disp} is the pre-fault scheduled active power reference, u^+ is the positive sequence voltage magnitude at the inverter point of common coupling (PCC), k_{isp} and u^+_{ref} are respectively the droop gain and voltage reference for positive sequence contribution.
- **Inverter Current Saturation:** According to most grid-code requirements, PV inverter typically prioritizes the reactive current in positive sequence over the active current when it reaches the inverter current limitation during the fault. This reactive current prioritization can be formulated as follows:

$$\begin{cases} i^+_d = \min[i^+_{dref}, i_{\max}] \\ i^+_q = \min[i^+_{qref}, \sqrt{i^2_{\max} - {i^+_d}^2}] \end{cases} \tag{5}$$

where $i_{\max}$ is the nominal current of the PV inverter, i^+_{dref} and i^+_{qref} are the reactive and active current references generated by the outer control loop as per (4) respectively, i^+_d and i^+_q are the actual reactive and active current injection from the PV inverter considering current saturation, respectively.

III. Case Studies

In this work, the test system under study includes a grid-connected PVPP with 48 PV inverters and a string MV collection grid, as shown in Fig. 1. The parameters used to model the swing equation are shown in Table I of the Appendix Section, while other parameters of the system under study can be found in [17]. MATLAB Simulink platform is used to perform EMT simulation studies on the test system shown in Fig. 1. In particular, two simulation scenarios are considered to investigate the impact of fault location on the extent of subsequent voltage-induced frequency disturbance: the upstream fault and the downstream fault, as marked in Fig. 1.

A. Voltage-induced Frequency Disturbance Analysis Following Upstream Short-circuit Faults

Short-circuit analysis is performed with an upstream fault location at the high voltage transmission grid. To investigate the impact of fault type of the extent of subsequent voltage-induced frequency disturbance, three different fault types are simulated, as follows: balanced three-phase-to-ground (3P2G)

979-8-3315-8138-1

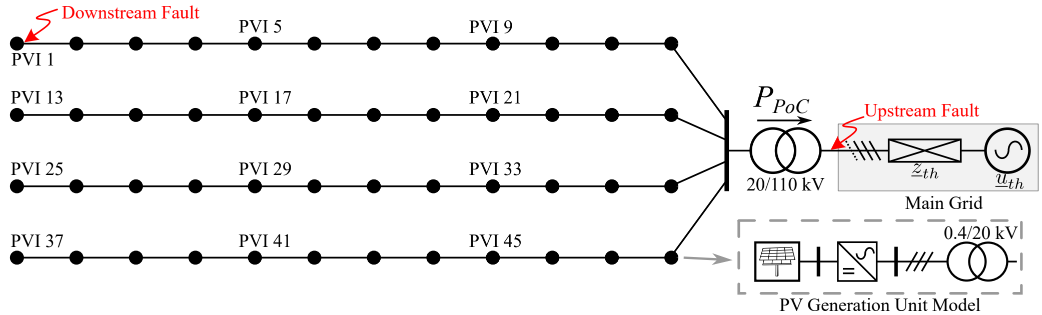

Fig. 1. The system under study og a grid-connected PVPP with 48 PV inverters and a string MV collection grid.

fault, phase-to-phase (P2P) fault, and single-phase-to-ground (1P2G) fault. The EMT simulation results are obtained and respectively demonstrated in Fig. 2, Fig. 4, and Fig. 5. In these simulation results, we represent the active power injection measured from the PVPP PoC, as well as the grid frequency dynamics, following a given short-circuit fault.

The short-circuit fault is modeled considering an impedance of $j0.001$ pu at the upstream fault location at the time of 0.3 s. The fault is cleared later at the time of 0.6 s. Given the voltage sag across the system following the fault, all PV inverters hit their current limits and reduce the active power injections, which triggers the grid frequency dynamics.

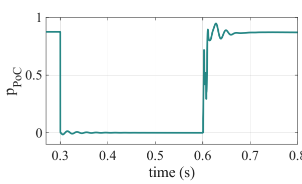

(a) PVPP Power Injection

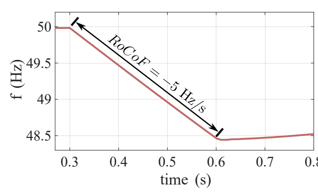

(b) Frequency

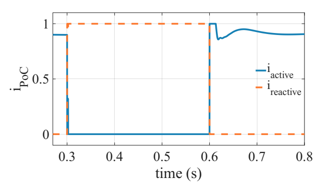

(c) PVPP Current Injection

Fig. 2. EMT simulation results considering the 3P2G upstream fault.

In particular, 3P2G fault represents the most critical case where the PVPP active power injection falls to zero during the fault, as shown in Fig. 2. This is because all PV inverters prioritize the reactive current injection over their active power so as to support the grid voltage during the fault, resulting in zero active power injection due to the inverter current limitation as per in (4) and (5), which can be observed from the active and reactive current injection from the PVPP at the PoC as shown in Fig. 2(c).

As a result, the system frequency exhibits a significant excursion with a frequency nadir of 48.5 Hz, which can potentially trigger secondary photovoltaic tripping (SVPT) protection on PV inverters and cause under-frequency-dependent PV shedding [18], [19]. This is especially critical for legacy inverters as they cannot withstand a severe under frequency event [20]. On the other hand, the high RoCoF of -5 Hz/s observed on the frequency dynamics is unlikely to trigger the protective tripping of PV inverters as the RoCoF-based protection is typically implemented with a $500-1000$ ms sliding window on their measurement unit [21]. However, it highlights the need for a timely fault clearance and a quick active power recovery following sever faults to prevent power interruption for a longer period.

The frequency dynamics of the system under study would also depend on the fault level available in the system, as per the simulation results shown in Fig. 3 with different fault impedance values considering a 3P2G fault at the upstream network. This is since the grid voltage still remain close to the nominal value when there is enough voltage stiffness behind an impedance, which allows PV inverters to inject certain amounts of active power during the fault according to their grid support control and current limitation.

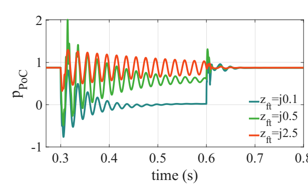

(a) PVPP Power Injection

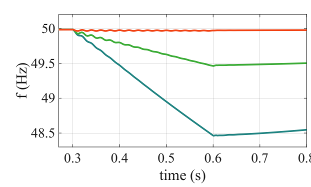

(b) Frequency

Fig. 3. Simulation results demonstrating the impacts of fault impedance on PVPP power injection and grid frequency.

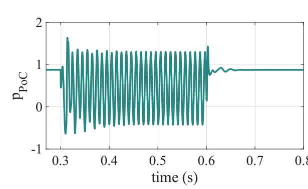

(a) PVPP Active Power Injection

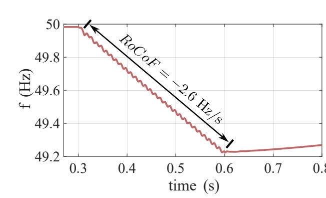

(b) Frequency

Fig. 4. EMT simulation results considering the P2P upstream fault.

Compared to the 3P2G fault case, the grid frequency shows a less significant excursion following unbalanced faults (P2P

979-8-3315-8138-1

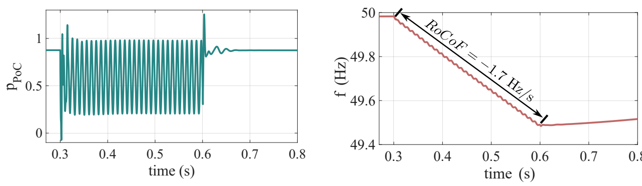

(a) PVPP Active Power Injection (b) Frequency

Fig. 5. EMT simulation results considering the 1P2G upstream fault.

and 1P2G), as per the simulation results shown in Fig. 4 and Fig. 5. This is since there is still enough inverter capacity for the PV unit to inject active power, given a higher voltage level in positive sequence at the PVPP PoC. In particular, the 1P2G fault case study results show the most moderate impact on grid frequency among the three fault cases represented in this paper. It is interesting to note the second-order oscillation on the PVPP active power (as well as the resulted frequency dynamics) due to the existence of negative sequence voltage during an asymmetrical fault, which might trigger further PV tripping and thus endanger the whole-system stability (e.g., PLL instability and DC voltage ripple) [22].

The test with a P2P fault as shown in Fig. 4 has been repeated considering a different control strategy on PVIs, prioritizing negative sequence current injection current, which is proportional to the negative sequence voltage magnitude, over the positive sequence, as per the recent grid-codes by system operators. According to the simulation results shown in Fig. 6, there is a chance of higher frequency excursions and RoCoF when IBRs are equipped with negative sequence current injection control. This is since the grid support control in negative sequence further reduces the room for positive sequence current injection from IBRs during the fault.

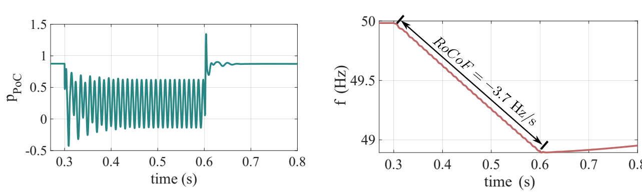

(a) PVPP Active Power Injection (b) Frequency

Fig. 6. EMT simulation results considering the P2P upstream fault with negative sequence current support from PVIs.

In light of the above, it becomes clear that voltage-induced frequency disturbances carry a significant risk of triggering cascading failures within the power system. This underscores the importance of developing a deeper understanding of the mechanisms behind these phenomena, as well as their potential to compromise system stability.

B. Voltage-induced Frequency Disturbance Analysis Following Downstream Short-circuit Faults

To further investigate the impact of fault location in voltage-induced frequency disturbances, short-circuit analysis is performed considering a downstream fault location at the MV collection grid, as highlighted in Fig. 1. In this case, only the balanced 3P2G fault is examined, as it is regarded as the most critical scenario. As discussed earlier in the upstream fault case study, this type of fault typically produces the most severe frequency excursions, making it the most suitable case for assessing the system stability under extreme conditions.

The results obtained from EMT simulation are shown in Fig. 7 following the downstream 3P2G fault occurrence. It is of interest to note that the active power injection from the PVPP drops below zero during the fault. As a result, the fault-induced frequency excursion involves a higher RoCoF of -7.3 Hz/s and a frequency nadir point of 47.8 Hz.

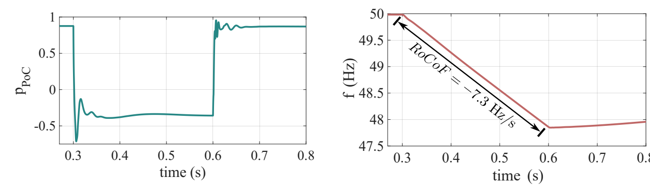

(a) PVPP Active Power Injection (b) Frequency

Fig. 7. EMT simulation results considering the 3P2G downstream fault.

It is worth noting that not all PV inverters operate with zero active current injection during their fault ride-through operation. This is evident from the current-saturation states observed during the downstream fault, as illustrated in Fig. 8. The red points refer to PV inverters with zero active power injection during the fault. In particular, only those PV inverters in the faulty string and close to the fault location are fully saturated, injecting zero active power during the fault. Although most PV inverters continue to inject active power, the fault current supplied by the main AC grid to the downstream fault location causes significant active power losses in the MV collection grid cables, which are predominantly resistive elements. Consequently, during the fault, these active power losses become large enough to reverse the direction of active power flow at the PVPP PoC.

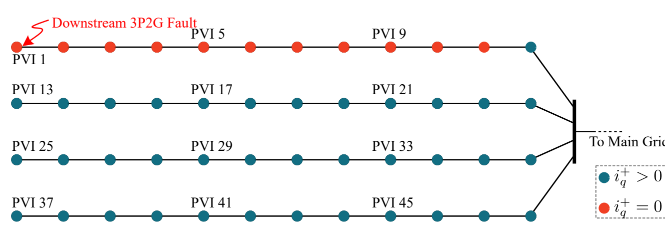

Fig. 8. Inverters' current saturation states during the downstream fault.

IV. Conclusion

This paper investigated voltage-induced frequency disturbances, referring to the subsequent frequency excursions that arise from the active power reduction of IBRs during an initial severe voltage disturbance and their corresponding fault ride-through operation. In particular, the study clarified how both

979-8-3315-8138-1

the fault type and the fault location influence the severity of this phenomenon. Performing EMT studies considering different fault types located at high-voltage upstream network, the following points are to be noted: *i* Severe frequency excursions can happen following short-circuit faults due to IBR active power reduction from their fault ride-through operation, reactive power prioritization, and the inverter current saturation. The severity of the subsequent frequency disturbance depends on how much inertia and frequency control ancillary services (FCAS) already available on the upstream network. This highlights the importance of inertia/FCAS procurement and a quick IBR active power recovery following fault clearance to mitigate the adverse impacts of voltage-induced frequency disturbances. Our simulation studies also highlighted the issue of possible IBR active power oscillations during their fault ride-through operation following unbalanced faults, mainly due to the presence of negative sequence voltage. This can potentially result in further inverter tripping and increase the likelihood of cascading failures. The analysis of the downstream fault indicated that the active power losses in the MV collection grid within the IBR plant can become substantial. These losses may lead to a reverse active power flow condition during the IBR fault ride-through operation, potentially resulting in non-compliance issues with performance requirements. All these complexities and operational risks should be noted by system operators and IBR project developers, particularly in power systems with low system strength and low inertia conditions.

Further investigation is required to account for the influence of grid-forming control mechanisms on the extent of voltage-induced frequency phenomena, which are becoming increasingly prevalent in modern power systems. Also, further comprehensive studies can be carried out considering different fault locations and grid topologies. In addition, extended investigation can be performed to assess the impact on grid transient stability from the reported voltage-induced frequency dynamics such as DC voltage stability and PLL stability.

APPENDIX

Table I presents the main grid parameters in the system under study in this paper, while other model parameters can be found in [17].

TABLE I
MAIN GRID PARAMETERS IN THE STUDIED SYSTEM

Parameter	Value	Parameter	Value
SCR	4 pu	p_0	-0.876 pu
D_{eq}	0.5 pu	H_{eq}	4 s
k_{pf}	50 pu	τ_{eq}	5 s

REFERENCES

[1] Y. Gu and T. C. Green, “Power system stability with a high penetration of inverter-based resources,” *Proceedings of the IEEE*, vol. 111, no. 7, pp. 832–853, 2023.

[2] R. Mittal, Z. Miao, L. Fan, *et al.*, “Oscillation risks of grid-following and grid-forming inverter-based resources in series-compensated networks,” *IEEE Transactions on Power Delivery*, vol. 40, no. 4, pp. 2426–2438, 2025.

[3] A. Azizi and A. Hooshyar, “Fault current limiting and grid code compliance for grid-forming inverters—part i: Problem statement,” *IEEE Transactions on Sustainable Energy*, vol. 15, no. 4, pp. 2486–2499, 2024.

[4] “IEEE Standard for Interconnection and Interoperability of Inverter-Based Resources (IBRs) Interconnecting with Associated Transmission Electric Power Systems,” *IEEE Std 2800-2022*, pp. 1–180, 2022.

[5] Q. Liu, K. Jia, B. Yang, *et al.*, “Analytical model of inverter-interfaced renewable energy sources for power system protection,” *IEEE Transactions on Power Delivery*, vol. 38, no. 2, pp. 1064–1073, 2023.

[6] M. Carreño, J. Song, O. Gomis-Bellmunt, and R. Griñó, “Design-oriented large-signal stability analysis of synchronous reference frame phase-locked loop,” *IEEE Transactions on Power Delivery*, vol. 40, no. 3, pp. 1235–1243, 2025.

[7] Z. Zeng, D. Yang, H. Wu, *et al.*, “A direct current-synchronization control for voltage source converter with enhanced fault ride-through capability,” *IEEE Open Journal of Power Electronics*, vol. 5, pp. 1484–1499, 2024.

[8] J. Song, J. Arévalo-Soler, M. Cheah-Mane, *et al.*, “Dynamic equivalent representation for symmetrical short-circuit analysis of power systems with power electronics,” *Electric Power Systems Research*, vol. 235, p. 110657, 2024.

[9] M. Zhang, Y. Lv, F. Xue, *et al.*, “Voltage-frequency interaction mechanism under short-circuit faults in a high proportion of new energy-receiving grids,” in *2025 4th International Conference on New Energy System and Power Engineering (NESP)*, pp. 679–686, 2025.

[10] D. Lekshmi J., Z. H. Rather, and B. C. Pal, “Voltage-dip induced frequency excursions in solar pv power integrated power system,” in *2020 IEEE International Conference on Power Systems Technology (POWERCON)*, pp. 1–6, 2020.

[11] H. Andrew, “System strength in islanded powr systems and relation with inertia,” in *AEMO CIGRE System Strength Workshop*, pp. 1–12, 2020.

[12] NESO, “Voltage and frequency dependency.” https://www.neso.energy/document/118651/download, 2018.

[13] C. Hao, L. Wei, Q. Zhaohui, *et al.*, “Grid frequency trajectory fitting under transient power impact caused by highly proportional wind power fault ride,” in *2023 IEEE International Conference on Power Science and Technology (ICPST)*, pp. 108–116, 2023.

[14] Z. Rather and D. Flynn, “Impact of voltage dip induced delayed active power recovery on wind integrated power systems,” *Control Engineering Practice*, vol. 61, pp. 124–133, 2017.

[15] H. Karbouj and Z. H. Rather, “A novel wind farm control strategy to mitigate voltage dip induced frequency excursion,” *IEEE Transactions on Sustainable Energy*, vol. 10, no. 2, pp. 637–645, 2019.

[16] M. M. Kabsha and Z. H. Rather, “Advanced lvrt control scheme for offshore wind power plant,” *IEEE Transactions on Power Delivery*, vol. 36, no. 6, pp. 3893–3902, 2021.

[17] J. Song, M. Cheah-Mane, E. Prieto-Araujo, and O. Gomis-Bellmunt, “Short-circuit calculation of power systems with power electronics converters considering asymmetrical faults and converter limits,” *International Journal of Electrical Power & Energy Systems*, vol. 170, p. 110804, 2025.

[18] M. G. Dozein, G. Chaspierre, and P. Mancarella, “Contribution to system frequency stability and resilience from pv plants: A closed-loop system identification approach,” in *2020 55th International Universities Power Engineering Conference (UPEC)*, pp. 1–6, 2020.

[19] M. G. Dozein, G. Chaspierre, P. Mancarella, *et al.*, “Frequency response from solar pv: A dynamic equivalence closed-loop system identification approach,” *IEEE Systems Journal*, vol. 16, no. 1, pp. 713–722, 2022.

[20] AEMC, “National electricity rules v87.” https://energy-rules.aemc.gov.au/ner/668, 2016.

[21] A. Khashei, M. G. Dozein, and R. Razzaghi, “Der tripping in distribution networks: Root causes and classification framework,” *Sustainable Energy, Grids and Networks*, vol. 43, p. 101824, 2025.

[22] A. Junyent-Ferre, O. Gomis-Bellmunt, T. C. Green, *et al.*, “Current control reference calculation issues for the operation of renewable source grid interface vscs under unbalanced voltage sags,” *IEEE Transactions on Power Electronics*, vol. 26, no. 12, pp. 3744–3753, 2011.

979-8-3315-8138-1